Journal of Proteomics 241 (2021) 104242

Contents lists available at ScienceDirect

Journal of Proteomics

journal homepage: www.elsevier.com/locate/jprot

Integrated transcriptome and proteome analysis reveals potential mechanisms for differential abdominal fat deposition between divergently selected chicken lines

Lijian Wang [a,b,c,1], Li Leng [a,b,c,1], Ran Ding [a,b,c], Pengfei Gong [a,b,c], Chang Liu [a,b,c], Ning Wang [a,b,c], Hui Li [a,b,c], Zhi-Qiang Du [a,b,c,*], Bohan Cheng [a,b,c,*]

[a] Key Laboratory of Chicken Genetics and Breeding, Ministry of Agriculture and Rural Affairs, Harbin 150030, PR China
[b] Key Laboratory of Animal Genetics, Breeding and Reproduction, Education Department of Heilongjiang Province, Harbin 150030, PR China
[c] College of Animal Science and Technology, Northeast Agricultural University, Harbin 150030, PR China

ARTICLE INFO

Keywords:
Fat deposition
Transcriptome
Proteome
Chicken
Adipose tissue

ABSTRACT

Genetic selection for meat production performance of broilers concomitantly causes excessive abdominal fat deposition, accompanied by several adverse effects, such as the reduction of feed conversion efficiency and reproduction performance. Our previous studies have identified important genes regulating chicken fat deposition, using the Northeast Agricultural University broiler lines divergently selected for abdominal fat content (NEAUHLF) as an animal model. However, the molecular mechanism underlying fat deposition differences between fat and lean broilers remains largely unknown.

Here, we integrated the transcriptome (RNA-Seq) and quantitative proteome (isobaric tags for relative and absolute quantitation, iTRAQ) profiling analyses on abdominal fat tissues from NEAUHLF chicken lines. Differentially expressed genes (2167 DEGs, corrected p-value < 0.01) and differentially abundant proteins (199 DAPs, corrected p-value < 0.05) were identified in lean line compared to fat line. Down-regulated DEGs and DAPs mainly enriched in pathways related to fatty acid metabolism, fatty acid biosynthesis, and PPAR signaling, and interestingly, up-regulated DEGs and DAPs enriched both in lysosome pathway. Moreover, numerous key DEGs and DAPs involved in long-chain fatty acid uptake, *in situ* lipogenesis (fatty acid and cholesterol synthesis), and lipid droplet accumulation were discovered after integrated transcriptome and proteome analysis.

Significance: Excessive abdominal fat deposition critically affects the health of broilers and causes economic loss to broiler producers, but the molecular mechanism of abdominal fat deposition is still unclear in chicken. We identified key DEGs/DAPs and potential pathways through an integration of chicken abdominal fat tissues transcriptome and proteome analyses. Our findings will facilitate a better revealing the mechanism and provide a novel insight into abdominal fat content discrepancy between the fat and lean chicken lines.

Abbreviations: ACACA, acetyl-CoA carboxylase alpha; ACADL, acyl-CoA dehydrogenase long chain; ACAT1, acetyl-CoA acetyltransferase 1; ACOX1, acyl-CoA oxidase 1; ACP5, acid phosphatase 5, tartrate resistant; ACSBG1, acyl-CoA synthetase bubblegum family member 1; ACSL1, acyl-CoA synthetase long-chain family member 1; ADIPOQ, adiponectin, C1Q and collagen domain containing; ANGPT1, angiopoietin 1; ARL6IP5, ADP ribosylation factor like GTPase 6 interacting protein 5; ARSB, arylsulfatase B; ATP6V0D2, ATPase H^+ transporting V0 subunit d2; CAV1, caveolin 1; CLTA, clathrin light chain A; CTSC, cathepsin C; CTSD, cathepsin D; CTSH, cathepsin H; CTSS, cathepsin S; CTSV, cathepsin V; DNASE2B, deoxyribonuclease 2 beta; EPHX2, epoxide hydrolase 2, cytoplasmic; FADS2, fatty acid desaturase 2; FASN, fatty acid synthase; GLA, galactosidase alpha; GM2A, GM2 ganglioside activator; GNS, glucosamine (N-acetyl)-6-sulfatase; GSTT1L, glutathione S-transferase theta 1-like; HACD1, 3-hydroxyacyl-CoA dehydratase 1; HACD2, 3-hydroxyacyl-CoA dehydratase 2; HEXB, hexosaminidase subunit beta; HSD17B4, hydroxysteroid 17-beta dehydrogenase 4; HSD17B7, hydroxysteroid 17-beta dehydrogenase 7; LAPTM5, lysosomal protein transmembrane 5; LITAF, lipopolysaccharide induced TNF factor; LPL, lipoprotein lipase; NAGA, alpha-N-acetylgalactosaminidase; MAP4, microtubule associated protein 4; MAPK6, Mitogen-activated protein kinase 6; OXSM, 3-oxoacyl-ACP synthase, mitochondrial; PLIN1, perilipin 1; PLIN4, perilipin 4; PPT1, palmitoyl-protein thioesterase 1; POR, cytochrome p450 oxidoreductase; PRDX6, peroxiredoxin 6; RETSAT, retinol saturase; SFTPA1, surfactant protein A1; SLC11A1, solute carrier family 11 member 1; SLC27A6, solute carrier family 27 member 6; VAT1, vesicle amine transport 1.

* Corresponding authors. College of Animal Science and Technology, Northeast Agricultural University, Harbin 150030, PR China.
E-mail addresses: zhqdu@neau.edu.cn (Z.-Q. Du), chengbohan1027@126.com (B. Cheng).

[1] Lijian Wang and Li Leng contributed equally to this work and should be regarded as joint first authors.

https://doi.org/10.1016/j.jprot.2021.104242
Received 4 January 2021; Received in revised form 18 April 2021; Accepted 19 April 2021
Available online 23 April 2021

1. Introduction

The meat-type chickens (broilers) have been intensively selected for fast growth rate and better feed efficiency over the past 70 years. As the most efficient animal production system, broilers can provide cheap and nutritious animal protein for human consumption. In the meantime, with broiler's fast growth, series of problems also occur such as the decline in physiological adaptability, especially abdominal fat deposition. The excessive deposition of abdominal fats is not only unfavorable to the health of broilers, but also causing a huge economic loss to broiler producers [1]. Consequently, to solve excessive abdominal fat deposition is still an urgent task for broiler breeders all over the world.

Fat deposition in chickens is a complex quantitative trait regulated by multiple genetic (*e.g.*, epistasis [2,3]) and environmental factors (*e.g.*, ambient temperature and lighting regimes [4–6]). For poultry, the liver is generally considered to be the main site for *de novo* synthesis of fatty acids, and these fatty acids are synthesized to triglycerides in the liver and then transported to other tissue (*e.g.*, adipose tissue) for use [7]. In fact, the adipose tissue is normally regarded as the main organ to deposit fat, and the liver-derived triglycerides could be re-esterified and deposited in the adipose tissue [8]. Since 1996, we established two broilers lines based on divergent selection on abdominal fat percentage and plasma very low-density lipoprotein (VLDL) concentration (NEAUHLF) [9], which is an ideal model for studying the molecular basis of adipose tissue growth and development. As a result, we have discovered a number of key genes underlying fat deposition through microarray [10,11] and two-dimensional gel electrophoresis technologies, such as adipocyte fatty acid binding protein (A-FABP) and Apolipoprotein A-I (Apo-AI) [12,13]. However, the molecular mechanism for abdominal fat deposition differences between fat and lean broiler lines remains unclear.

Recently, with the development of high-throughput sequencing technology, integration of transcriptome and proteome technologies has become an important means and routine to analyze the molecular mechanism of agricultural complex traits in farm animals [14–16]. In the present study, we examined the differences of transcriptome and quantitative proteome profiling on abdominal adipose tissues between the two broiler lines at 7 weeks of age. We identified numerous key DEGs and DAPs potentially involved in long-chain fatty acid uptake, *in situ* lipogenesis (fatty acid and cholesterol synthesis), and lipid droplets accumulation, facilitating our understanding of abdominal fat content differences between chicken lines under divergent selection.

2. Materials and methods

2.1. Animals and samples preparation

Animal work was conducted according to the guidelines for the care and use of experimental animals established by the Ministry of Science and Technology of the People's Republic of China (approval number: 2006–398), and was approved by the Laboratory Animal Management Committee of Northeast Agricultural University (Harbin, China). The experimental birds were obtained from the Avian Farm of Northeast Agricultural University (Harbin, Heilongjiang, China). These broilers under divergent selection over 19 generations were employed from Northeast Agricultural University broiler lines divergently selected for high and low abdominal fat content (NEAUHLF), exhibiting a large difference in abdominal fat content as previously described [9]. In total, ten male birds (lean line, n = 5, and fat line, n = 5) at 7 weeks of age from the 19th generation of NEAUHLF were used for RNA-seq and iTRAQ analysis, and these birds were kept under the same environmental conditions and had free access to feed and water. Abdominal fat tissues were collected right after these birds were euthanized by intramuscular injection of pentobarbital (Sigma, St. Louis, MO, USA; 40 mg/kg) under deep anesthesia, and then immediately frozen in liquid nitrogen and stored at −80 °C. The detailed information of selected chickens' abdominal fat weight and abdominal fat percentage were showed in Fig. 1a and b.

2.2. Transcriptomic data collection and analysis

Total RNA from abdominal fat tissues was extracted using the TRIzol reagent (Invitrogen, New Jersey, NJ, USA), and genomic DNA was removed by DnaseI treatment. RNA purity, concentration and integrity were checked by NanoPhotometer® spectrophotometer (IMPLEN, CA, USA), Qubit® RNA Assay Kit in Qubit® 2.0 Flurometer (Life Technologies, CA, USA), and RNA Nano 6000 Assay Kit of the Bioanalyzer 2100 system (Agilent Technologies, CA, USA), respectively. After removal of ribosomal RNA and cleaning-up of rRNA free residue by a Ribo-Zero™ rRNA Removal Kit (Epicentre, USA), the sequencing libraries were generated using the NEBNext® Ultra™ Directional RNA Library Prep Kit for Illumina® (NEB, USA) following the manufacturer's recommendations. cDNA fragments of 150–200 bp in length were selected and purified with the AMPure XP system (Beckman Coulter, Beverly, USA). Then, library quality was assessed by the Agilent Bioanalyzer 2100 system, and results showed that the RNA integrity number (RIN) of these samples ranged from 8.6 to 9.2 (Table S1). Finally, after cluster generation (cBot Cluster Generation System using TruSeq PE Cluster Kit v3-cBot-HS, Illumina), the libraries were sequenced on an Illumina Hiseq 4000 platform, and 150 bp paired-end reads were produced.

After demultiplex and quality filtering of raw data, clean reads were obtained and aligned to the *G. gallus* 6.0 reference genome assembly using HISAT2 (v.2.0.4) [17]. The mapped reads of each sample were assembled and quantified by StringTie (v1.3.1) [18] in a reference-based approach. And differentially expressed genes were identified by DESeq2 [19]. Genes with a corrected p-value < 0.01 and fold changes >1.5 or < 0.67 were assigned as significantly differentially expressed.

2.3. Proteomics

Protein was extracted according to Damerval et al. [20], checked by SDS-PAGE (Fig. S1) and concentration was determined by the Bradford method [21]. Following reduction, cysteine alkylation, and trypsin digestion, total proteins were treated to obtain peptides, and labeled with iTRAQ 8-plex or iTRAQ 4-plex reagents (AB SCIEX, USA), as 113 (LL1), 114 (LL2), 115 (LL3), 116 (LL4), 117 (LL5), 118 (FL1), 119 (FL2), and as 117 (FL3), 118 (FL4), 119 (FL5), respectively. We pooled all samples and labeled as 121 in 8-plex and 4-plex iTRAQ, to calibrate the two iTRAQ experimental data sets. Then, the iTRAQ-labeled peptide mixture was reconstituted and loaded on SCX (strong cation exchange) column, which were subjected to nanoelectrospray ionization, followed

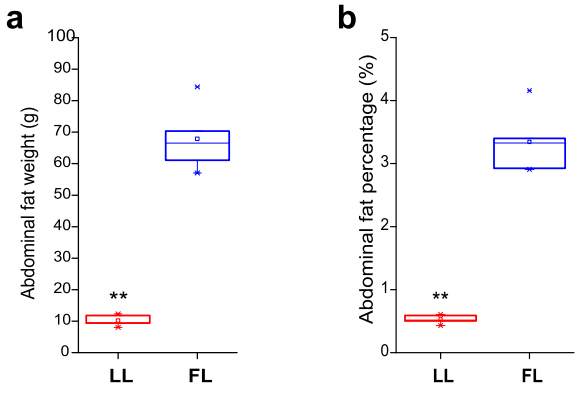

Fig. 1. Body measurement of selected chicken.
Chicken' abdominal fat weight (a) and abdominal fat percentage (b) were measured between fat and lean chicken lines (n = 5 for each line). Data were showed as mean ± SD. **Represents extremely statistically significant differences. FL and LL represent the fat and lean chicken lines, respectively.

by tandem mass spectrometry (MS/MS) in a TripleTOF 5600 system (AB SCIEX, USA).

The MS/MS data were processed with ProteinPilot Software v. 5.0 (AB SCIEX, USA) against *Gallus gallus* database using the Paragon algorithm [22]. The experimental data from tandem mass spectrometry (MS) were utilized to match the theoretical data to identify proteins, which was performed by the search option (with an emphasis on biological modifications). An automatic decoy database search strategy was used to estimate the false discovery rate (FDR) calculated as the false positive matches divided by total matches, using the PSPEP (Proteomics System Performance Evaluation Pipeline Software, integrated into the ProteinPilot Software). In order to correct the batch effect, the ComBat algorithm of 'sva' R package was used [23] (Fig. S2). The significantly differentially abundant proteins were identified using the following criteria: 1) peptide groups considered for quantification required at least 2 peptides, and a global FDR less than 1% was used; and 2) a fold change >1.5 or <0.67 and with corrected p-value < 0.05.

2.4. RT-qPCR analysis

To validate RNA-Seq results, 20 DEGs with higher expression levels and larger fold changes were validated by RT-qPCR. Ten male birds (n = 5 for each line) from the 19th generation of NEAUHLF were used. Total RNA from abdominal fat tissue was reversely transcribed into cDNA using a PrimeScript™ RT Reagent Kit (Takara, Dalian, China). FastStart Universal SYBR Green Master kit (Roche) and the ABI 7900 PCR detection system were used to perform RT-qPCR. The program began at 95 °C for 30 s for activation, followed by 40 cycles of amplification at 95 °C for 5 s and 58 °C for 30 s. An additional 15 s at 95 °C, 1 min at 60 °C, and 15 s at 95 °C were performed for the melt curve stage. The housekeeping gene TATA-Box binding protein (*TBP*) was used as the control. RT-qPCR primer pairs were designed by Primer Premier 6.0 and the detailed information were listed in Table S2. The comparative $2^{-\Delta\Delta Ct}$ method was used to determine the statistical significance.

2.5. Parallel reaction monitoring (PRM)-MS analysis

To verify the protein abundance level obtained by iTRAQ analysis, 10 DAPs with higher abundance levels and larger fold changes were selected for validation. Signature peptides for the target proteins were defined according to the iTRAQ data, and only were unique peptide sequences selected for the PRM-MS analysis (Table S3). We randomly selected 6 male birds from the 19th generation (n = 3 for each line) of NEAUHLF, and extracted the proteins from abdominal fat tissues, which were prepared following the iTRAQ protocol. Tryptic peptides were loaded on C18 stage tips for desalting prior to reversed-phase chromatography on an Easy nLC-1200 system (Thermo Scientific).

One-hour liquid chromatography gradients with acetonitrile ranging from 5 to 35% were used, and PRM was performed on a Q-Exactive Plus mass spectrometer (Thermo Scientific). Methods were optimized for collision energy, charge state, and retention times for the most significantly regulated peptides experimentally, using unique peptides of high intensity and confidence for each target protein. The mass spectrometer was operated in positive ion mode and with the following parameters: the full MS1 scan was acquired with the resolution of 70,000 (at 200 m/z), automatic gain control (AGC) target values 3.0×10^6, and a 250 ms maximum ion injection times. Full MS scans were followed by 20 PRM scans at 35000 resolution (at m/z 200) with AGC 3.0×10^6 and maximum injection time 200 ms. The targeted peptides were isolated with a 2.0 Th window and fragmented at a normalized collision energy of 27 in a higher energy dissociation (HCD) collision cell. The raw data were analyzed using Skyline (MacCoss Lab, University of Washington) [24] to get the signal intensities of individual peptide sequences.

For PRM MS data, each sample's average base peak intensity was extracted from the full scan acquisition using RawMeat (version 2.1, VAST Scientific). The normalization factor for sample N was calculated as f_N = the average base peak intensity of sample N divided by the median of average base peak intensities of all samples. The area under curve (AUC) of each transition from sample N was multiplied by this factor. After normalization, the AUC of each transition was summed to obtain AUCs at the peptide level. Relative protein abundance was defined as the intensity of a certain peptide.

2.6. Gene enrichment analysis

DEGs and DAPs were submitted for the gene ontology (GO) analysis by the clusterProfiler package [25], and the Kyoto Encyclopedia of Genes and Genomes (KEGG) pathway analysis (http://kobas.cbi.pku.edu.cn/kobas3). The thresholds for significant enrichment was set at corrected p-value < 0.05.

2.7. Statistical analysis

The p-value of DEGs, DAPs, GO term and KEGG pathway enrichment were adjusted by the Benjamini-Hochberg (BH) method. Chicken body measurement data were showed as mean ± SD. Two-tailed student's t-test was used to compare the differences between two groups, and the threshold of significance was set at $p < 0.05$.

3. Results

3.1. Transcriptome profiling

Ten male chickens with significant differences in abdominal fat weight and percentage were used to RNA-seq and iTRAQ analysis (Fig. 1a and b). RNA-Seq generated 77,841,982 to 95,203,262 raw reads for each library (Table S4). After filtering the low-quality reads, the average number of clean reads was 89,456,223 and 85,002,558 for the lean line (LL) and fat line (FL), respectively (Table S4). DESeq2 package was used to identify differentially expressed genes (DEGs) between LL and FL. Finally, 2167 DEGs with corrected p-value < 0.01 were found, of which 1058 were up-regulated and 1109 down-regulated in LL compared to FL (Fig. 2a and b and Table S5). To verify the accuracy of RNA-Seq data, 20 DEGs were chosen and their expression levels were assayed by RT-qPCR. Except for *MAPK6*, other genes showed consistent results for both RNA-Seq and RT-qPCR (Fig. 2c).

Then, the down- and up-regulated DEGs were enriched by GO and KEGG pathway analyses, respectively. GO analysis showed down-regulated DEGs significantly enriched in GO terms such as "oxidation-reduction", "anchored component of membrane", "respiratory chain complex" and "oxidoreductase activity" (Fig. 2d); up-regulated DEGs significantly enriched in GO terms such as "defense response", "response to external biotic stimulus" and "molecular function regulator"(Fig. 2e). The KEGG pathway analysis also revealed that down-regulated DEGs significantly enriched in 8 pathways, including "fatty acid metabolism", "PPAR signaling pathway", "steroid biosynthesis", "metabolic pathways", "wnt signaling pathway", "adherens junction" , "fatty acid biosynthesis" and "ABC transporters"; up-regulated DEGs significantly enriched in pathways such as "lysosome", "metabolic pathways" and "biosynthesis of amino acid" (Fig. 3a). Thus, transcriptome sequencing found that pathways related to fatty acid metabolism could be important in fat deposition differences in our divergently selected chicken lines.

3.2. iTRAQ-based proteomics

To better understand the potential mechanisms underlying differential abdominal fat deposition between fat and lean broilers, iTRAQ-based proteomics was also performed. Eight-plex iTRAQ generated 61,498 spectra and 18,672 unique peptides (matching to 2424 proteins); four-plex iTRAQ generated 45,203 spectra and 14,300 unique peptides (matching to 2185 proteins). After stringent selection of unique peptides (95% confidence limit and global FDR < 1%), we identified 2137 and

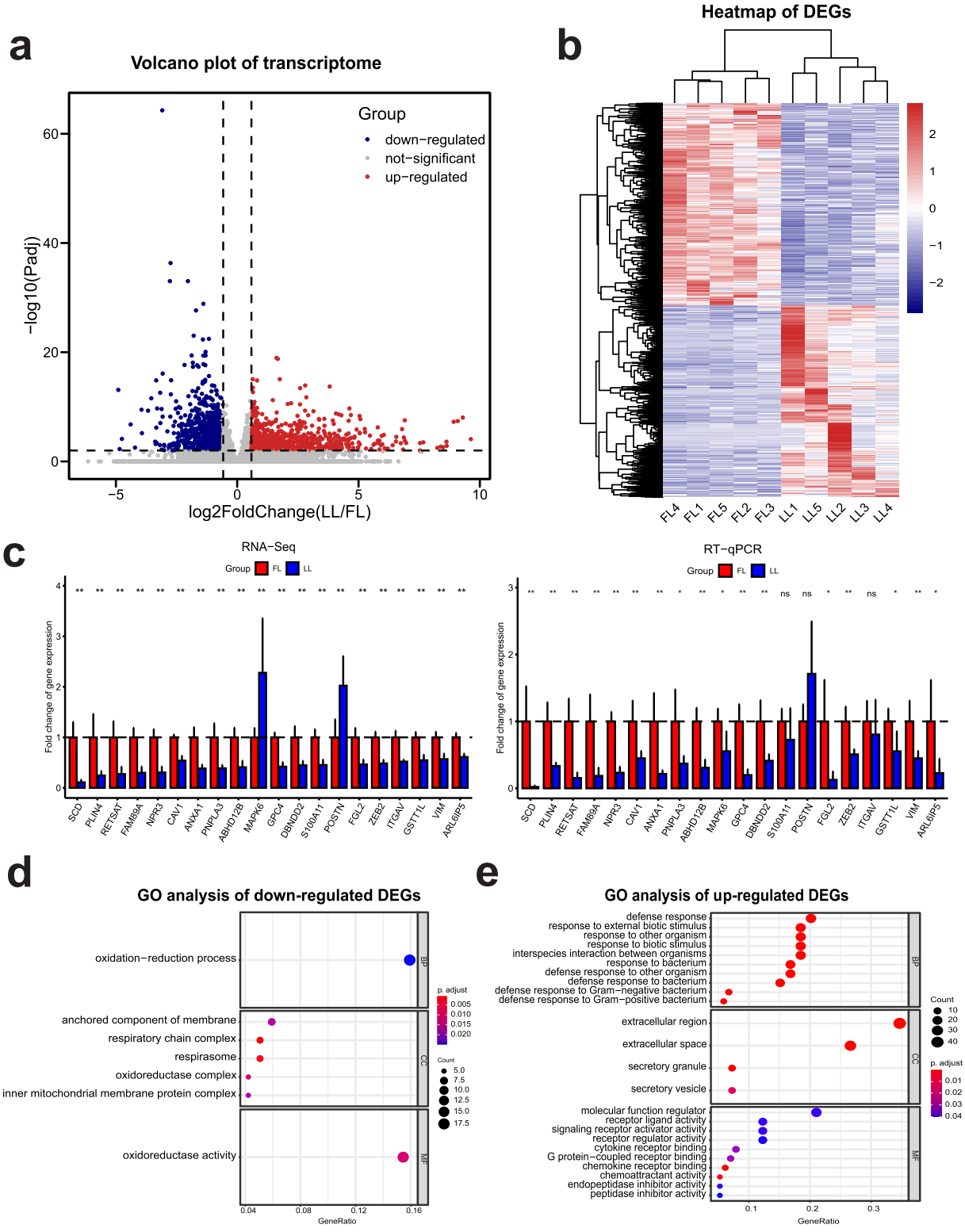

Fig. 2. Transcriptome analysis on abdominal fat tissues in fat and lean chicken lines.
(a) Volcano plot of differentially expressed genes (DEGs) in chicken abdominal fat tissues with RNA-Seq analyses between fat and lean chicken lines. X-axis shows $\log_2$(Fold Change), and Y-axis represents the -$\log_{10}$(Padj). The blue dots represent the significantly down-regulated DEGs, the red dots represent the significantly up-regulated DEGs, and the gray dots represent the not-significantly differentially expressed genes. (b) The heat map of hierarchical clustering of DEGs between the fat and lean chicken lines. FL and LL represent the fat and lean chicken lines, respectively. (c) The bar graph shows the expression level of selected genes detected by RNA-Seq (n = 5 for each line) and validated by RT-qPCR (n = 5 for each line). X-axis shows the gene symbols, and Y-axis shows the fold change of gene expression. Data were showed as mean ± SD. *Represents statistically significant differences, **represents extremely statistically significant differences, and ns represents statistically not-significant differences. (d) and (e) GO analysis of down- and up-regulated DEGs (corrected $p < 0.05$). X-axis shows gene ratio, and Y-axis shows GO terms. BP represents biological processes, CC represents cellular components, and MF represents molecular functions. (For interpretation of the references to colour in this figure legend, the reader is referred to the web version of this article.)

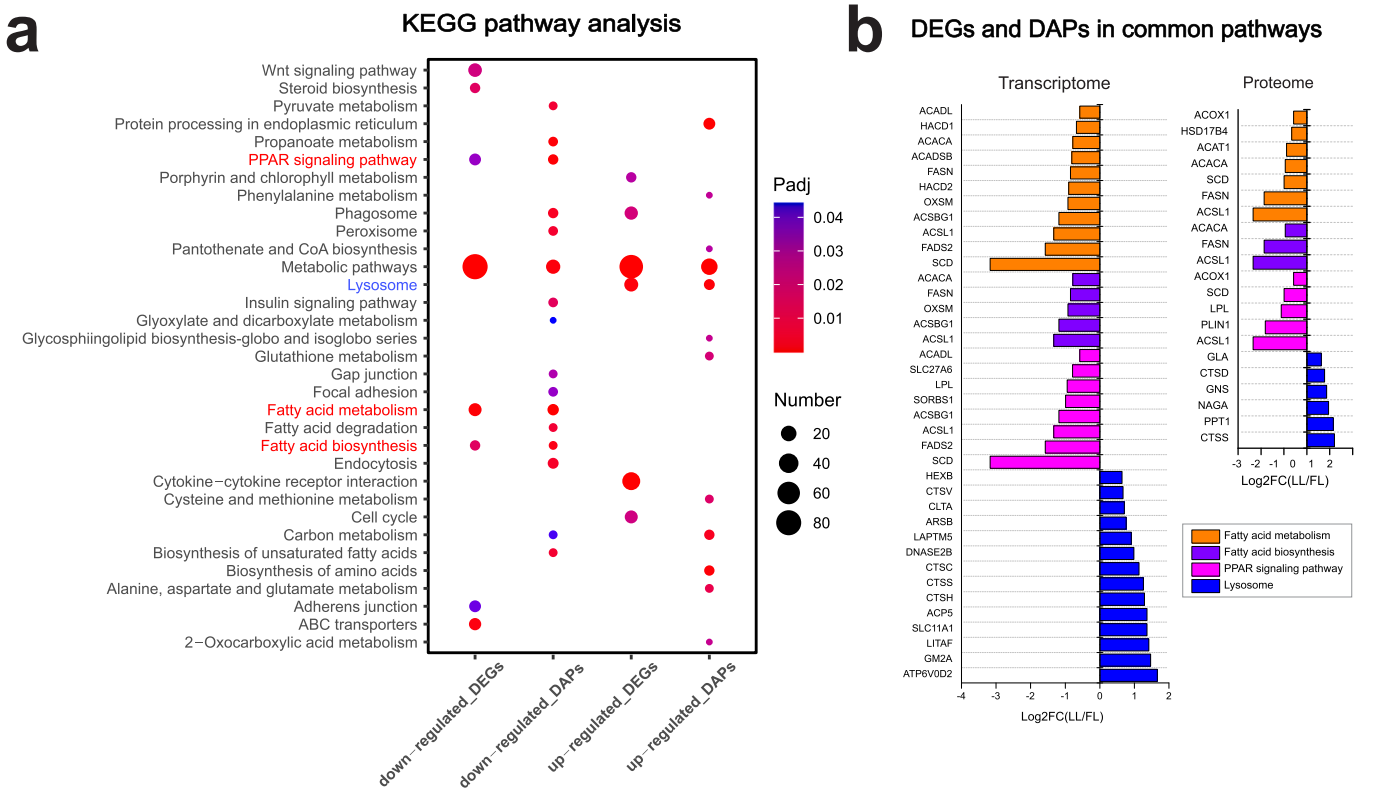

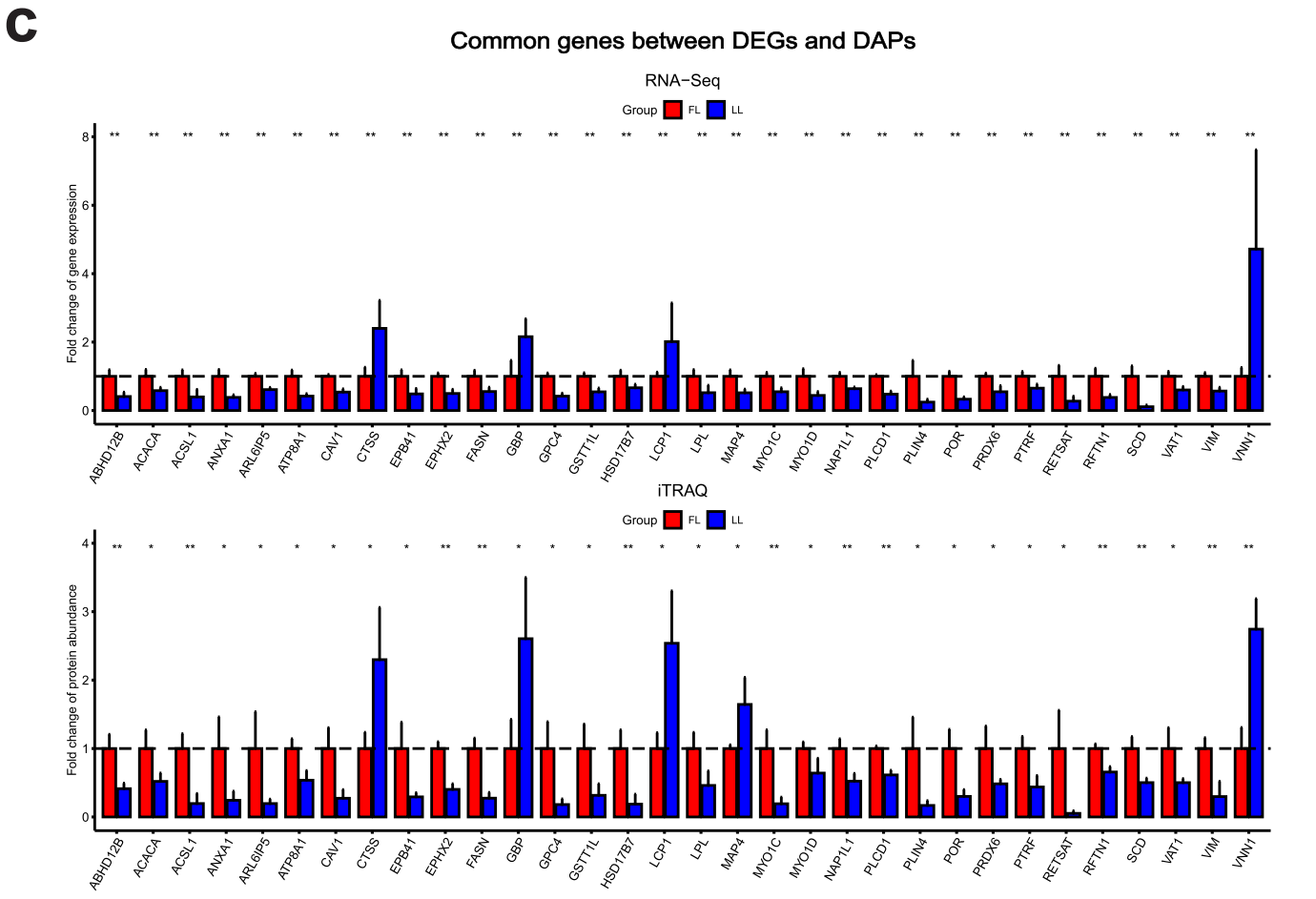

(caption on next page)

Fig. 3. Integrated analysis of transcriptome and proteome in chicken abdominal fat tissues.
(a) The KEGG pathway analysis of down- and up-regulated differentially expressed genes (DEGs) and differentially abundant proteins (DAPs) between the fat and lean chicken lines. (corrected $p < 0.05$). The blue pathway represents overlapped pathways that enriched by both up-regulated DEGs and DAPs, and the red pathways represent overlapped pathways that enriched by both down-regulated DEGs and DAPs. (b) The bar graph shows the regulation levels of DEGs and DAPs in the four overlapped pathways that related to lipid metabolism. X-axis shows log2(Fold Change), and Y-axis represents the gene symbols. (c) The bar graph shows the regulation trends of 32 shared genes at both the transcriptional and protein levels. X-axis shows the gene symbols, and Y-axis shows the fold change of gene expression or protein abundance. Data were showed as mean ± SD. *Represents statistically significant differences, **represents extremely statistically significant differences. (For interpretation of the references to colour in this figure legend, the reader is referred to the web version of this article.)

1727 proteins in the two iTRAQ experiments, respectively. Finally, 199 DAPs were identified between the two chicken lines, of which 109 were up-regulated and 90 down-regulated in LL compare to FL (Fig. 4a). The heat map of hierarchical clustering of DAPs was showed in Fig. 4b, and detailed information about every DAP was listed in Table S6. To validate the iTRAQ data, we selected 10 DAPs for the PRM analysis, and 9 of 10 proteins were successfully quantified. The PRM results of these nine proteins were consistent with our iTRAQ data (Fig. 4c).

Next, GO enrichment and KEGG pathway analysis were performed to determine the function of the down- and up-regulated DAPs. For the biological process (BP) category, "fatty acid biosynthetic process", "monocarboxylic acid biosynthetic process" and "fatty acid metabolic process" were significantly enriched by down-regulated DAPs (Fig. 4d). In addition, "endoplasmic reticulum lumen" and "calcium ion binding" were the most representative GO terms enriched by up-regulated DAPs for the cellular component (CC) and the molecular function (MF), respectively (Fig. 4e). KEGG pathway analysis showed that the down-regulated DAPs were mainly enriched in "metabolic pathways", and lipid metabolism-associated pathways, such as "PPAR signaling pathway", "insulin signaling pathway", "fatty acid biosynthesis", "biosynthesis of unsaturated fatty acids" and "fatty acid metabolism"; and up-regulated DAPs were significantly enriched in pathways such "metabolic pathways" and "lysosome" (Fig. 3a). In support of our transcriptome analysis, proteome analysis further discovered that pathways related to fatty acid metabolism are likely important in fat deposition differences between our fat and lean chicken lines.

3.3. Integrated transcriptome and proteome analysis

In order to further distinguish the critical DEGs and DAPs that may affect chicken abdominal fat deposition, integrated transcriptome and proteome analysis was conducted by combined analysis on our RNA-Seq and iTRAQ data. First, 32 overlapped genes were found by comparing the DEGs and DAPs. It was worth noting that except for *MAP4*, other genes show the same regulation tendency (Fig. 3c), suggesting these genes could be the key genes involved in the regulation of abdominal fat deposition.

Second, by comparing the pathways obtained after DEGs and DAPs enrichment analysis, except for the "metabolic pathways", we found that there were four overlapped pathways, three of which enriched by down-regulated DEGs and DAPs were related to lipid metabolism, such as "fatty acid metabolism", "PPAR signaling pathway", and "fatty acid biosynthesis", the only one enriched by both up-regulated DEGs and DAPs was "lysosome" (Fig. 3a and b), including 37 genes that may important for fat deposition. Together, 63 key DEGs/DAPs (32 significantly differentially regulated at both mRNA and protein levels, and 37 genes in overlapped pathways with ACACA, SCD, FASN, LPL, ACSL1, and CTSS appear twice) that may affect chicken abdominal fat deposition were discovered through our integrated transcriptome and proteome analysis (Table S7).

4. Discussion

Excessive accumulation of fat in adipose tissue easily leads to obesity and metabolic syndrome, such as insulin resistance, type 2 diabetes, heart disease, atherosclerosis and hypertension [26]. Exploring the molecular mechanism of adipose development and fat deposition is helpful for the therapy of obesity and related metabolic diseases.

Our fat and lean broilers have similar body weight but acquire a divergent abdominal fat content. So, it is the ideal animal model to study the molecular basis of fat deposition. In the current study, we combined RNA-Seq and iTRAQ techniques on abdominal adipose tissues from 7-week-old FL and LL broilers, and identified a number of key DEGs and DAPs that may affect fat deposition (Table S7). These genes are mainly involved in lipid metabolism associated processes, such as long-chain fatty acids uptake, *in situ* lipogenesis (fatty acid and cholesterol synthesis), and lipid droplet accumulation (Table 1).

4.1. Long-chain fatty acid uptake

In poultry, fatty acids are taken up by the adipose tissue, which mainly come from triglycerides in plasma lipoproteins (such as VLDL) synthesized and packaged by the liver, and also from triglycerides in portomicrons (PM) assembled by long-chain fatty acids in dietary fat [27]. The triglycerides contained in VLDL and PM are hydrolyzed by lipoprotein lipase located in adipose tissue-lined endothelial cells to produce free fatty acids, which can be taken up by adipocytes and then re-esterified and stored in lipid droplet as triglycerides [28]. Previous studies suggested that increased uptake of fatty acids in abdominal adipose tissue is a major cause of obesity in chickens [29]. In general, most cells show less ability in long-chain fatty acid uptake, whereas adipocytes and cardiomyocytes can efficiently and specifically absorb long-chain fatty acids [30]. In the present study, DEG (*CAV1*, *ACSL1*, and *SLC27A6*) and DAPs (LPL, CAV1, and ACSL1) were implicated in long-chain fatty acid uptake (Table 1). So, we speculate that long-chain fatty acid uptake may play an important role in chicken adiposity.

LPL is considered to be a rate-limiting enzyme in fat accretion in chicken adipose tissue [31], responsible for decomposing triglycerides in VLDL or PM to release free fatty acids. CAV1 was identified as the main plasma membrane fatty acid binding protein in adipocytes that can bind long-chain fatty acids with high affinity [32]. Lack of CAV1 results in the loss of caveolae and defects in long-chain fatty acid uptake in adipocytes [33]. In addition, CAV1 can bind to the long chain fatty acids on the inner leaflet of the lipid bilayer, and transport fatty acids to the subcellular membrane compartment through vesicle-mediated transport [34]. ACSL1 is an acyl-CoA synthetase, and functions as long-chain fatty acid transport protein in adipocyte [35]. The first step in using long-chain fatty acids in cells is their esterification reaction with CoA, and this reaction is catalyzed by acyl-CoA synthetase. In humans, there are two related long-chain fatty acid activation-related protein families: fatty acid transporters (FATP) and long-chain acyl-CoA synthetase (ACSLs). ACSL1 was found to co-localize with FATP1 in a small number of 3 T3-L1 cells [36]. Furthermore, ACSL1 can promote fatty acid uptake into cells depending on their expression levels [37,38]. *SLC27A6*, also named FATP6, is a kind of FATP that can enhance the uptake of long-chain and very-long-chain fatty acids into cells [39]. In the present study, the regulation levels of LPL, ACSL1, CAV1 and SLC27A6 were significantly higher in the FL adipose tissue, indicating the adipose tissues of the fat broilers have stronger long-chain fatty acid uptake ability to synthesize more triglycerides.

4.2. Fatty acids synthesis

The liver is widely considered to be the main site of *de novo* lipid

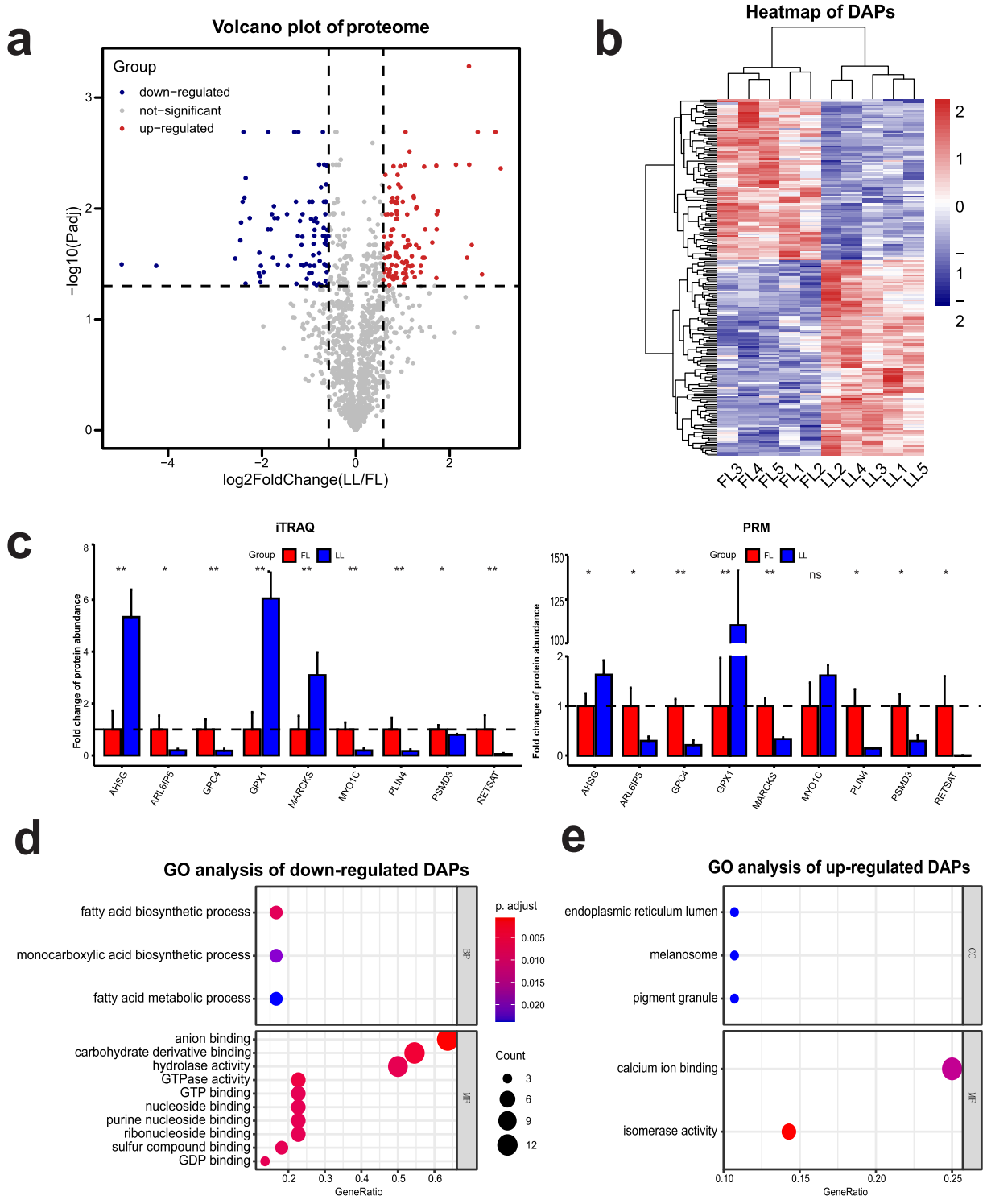

Fig. 4. Proteome analysis on abdominal fat tissues in fat and lean chicken lines.
(a) Volcano plot of differentially abundant proteins (DAPs) in chicken abdominal fat tissues with iTRAQ analyses between the fat and lean chicken lines. X-axis shows $\log_2$(Fold Change), and Y-axis shows $-\log_{10}$(Padj). The blue dots represent the significantly down-regulated DAPs, the red dots represent the significantly up-regulated DAPs, and the gray dots represent the not-significantly differentially abundant proteins. (b) The heat map of hierarchical clustering of DAPs between the fat and lean chicken lines. FL and LL represent the fat and lean chicken lines, respectively. (c) The bar graph shows the regulation level of selected proteins detected by iTRAQ (n = 5 for each line) and validated by PRM (n = 3 for each line). X-axis shows the gene symbols, and Y-axis shows the fold change of protein abundance. Data were showed as mean ± SD. *Represents statistically significant differences, **represents extremely statistically significant differences, and ns represents statistically not-significant differences. (d) and (e) GO analysis of down- and up-regulated DAPs (corrected $p < 0.05$). X-axis shows gene ratio, and Y-axis shows GO terms. BP represents biological processes, CC represents cellular components, and MF represents molecular functions. (For interpretation of the references to colour in this figure legend, the reader is referred to the web version of this article.)

Table 1
Genes related to lipid metabolism in chicken abdominal fat tissues.

Gene name	Gene symbol	Gene log2 (LL/FL)	Protein log2 (LL/FL)
Long-chain fatty acid uptake			
caveolin 1	CAV1	−0.8912	−1.8720
acyl-CoA synthetase long-chain family member 1	ACSL1	−1.3302	−2.3485
solute carrier family 27 member 6	SLC27A6	−0.7859	–
lipoprotein lipase	LPL	−0.9416	−1.1173
Fatty acid synthesis			
acetyl-CoA carboxylase alpha	ACACA	−0.7822	−0.9434
acyl-CoA synthetase bubblegum family member 1	ACSBG1	−1.1784	–
fatty acid desaturase 2	FADS2	−1.5794	–
fatty acid synthase	FASN	−0.8492	−1.8644
stearoyl-CoA desaturase (delta-9-desaturase)	SCD	−3.1763	−0.9940
3-hydroxyacyl-CoA dehydratase 1	HACD1	−0.6756	–
3-hydroxyacyl-CoA dehydratase 2	HACD2	−0.8972	–
acyl-CoA synthetase long-chain family member 1	ACSL1	−1.3302	−2.3485
3-oxoacyl-ACP synthase, mitochondrial	OXSM	−0.9256	–
acyl-CoA oxidase 1	ACOX1	–	−0.5798
hydroxysteroid 17-beta dehydrogenase 4	HSD17B4	–	−0.6621
Cholesterol synthesis			
epoxide hydrolase 2, cytoplasmic	EPHX2	−1.0052	−1.3117
cytochrome p450 oxidoreductase	POR	−1.5954	−1.7337
hydroxysteroid 17-beta dehydrogenase 7	HSD17B7	−0.5881	−2.4130
acetyl-CoA acetyltransferase 1	ACAT1	–	−0.8863
Lipid droplet accumulation			
perilipin 1	PLIN1	–	−1.8134
perilipin 4	PLIN4	−2.0249	−2.5699
caveolin 1	CAV1	−0.8912	−1.8720
Lysosome			
acid phosphatase 5, tartrate resistant	ACP5	1.3632	–
arylsulfatase B	ARSB	0.7599	–
ATPase H^+ transporting V0 subunit d2	ATP6V0D2	1.6667	–
clathrin light chain A	CLTA	0.7127	–
cathepsin C	CTSC	1.1374	–
cathepsin D	CTSD	–	0.7765
cathepsin H	CTSH	1.2896	–
cathepsin S	CTSS	1.2638	1.2010
cathepsin V	CTSV	0.6707	–
deoxyribonuclease 2 beta	DNASE2B	0.9856	–
galactosidase alpha	GLA	–	0.6289
GM2 ganglioside activator	GM2A	1.4721	–
glucosamine (N-acetyl)-6-sulfatase	GNS	–	0.8658
hexosaminidase subunit beta	HEXB	0.6435	–
lysosomal protein transmembrane 5	LAPTM5	0.9107	–
lipopolysaccharide induced TNF factor	LITAF	1.4160	–
alpha-N-acetylgalactosaminidase	NAGA	–	0.9444
palmitoyl-protein thioesterase 1	PPT1	–	1.1524
solute carrier family 11 member 1	SLC11A1	1.3671	–

synthesis in avian species, with more than 70% of *de novo* fatty acid synthesis occurring in liver tissue [40]. In addition to the liver, emerging evidence recently suggested that adipose tissue also plays a role in adiposity with a lipogenic activity, implying that the lipid synthesis ability of avian adipose tissue may be underestimated. Resnyk et al. [41] performed microarray analysis on 9-week-old chicken abdominal fat tissue and found many genes associated with lipogenesis were highly expressed in fat chicken. Similarly, one RNA-Seq analysis on 7-week-old broilers showed a large number of lipogenic genes were also up-regulated in abdominal adipose tissues from fat chicken [42]. Another RNA sequencing analysis showed that the 7-week-old fast growth chickens (fatter than slow growth chickens) over-express numerous lipogenic genes in adipose tissue, which should enhance *in situ* lipogenesis and ultimately adiposity [43]. Intriguingly, in the present study, we also found several key genes associated with fatty acids synthesis, including DEGs (*ACACA*, *FADS2*, *SCD*, *HACD1*, *HACD2*, *FASN*, *ACSL1*, *ACSBG1*, and *OXSM*) and DAPs (ACACA, FASN, SCD, ACSL1, ACOX1, and HSD17B4) (Table 1). KEGG analysis showed that ACACA, OXSM, FASN, ACSBG1 and ACSL1 were enriched in fatty acid biosynthesis pathway, and FADS2, SCD, HACD1, HACD2, HSD17B4 and ACOX1 were enriched in the biosynthesis of unsaturated fatty acids pathway (Fig. 3b and Table S7). It is worth noting that two proteins (ACACA and SCD) can work as critical enzymes to synthesize fatty acids. ACACA is the rate-limiting enzyme in fatty acid biosynthesis, which can catalyze the synthesis of malonyl-CoA from two molecules of acetyl-CoA, and produce fatty acids under the action of fatty acid synthase [44]. SCD is a rate-limiting enzyme that catalyzes the formation of monounsaturated fatty acids from saturated fatty acids [45].

Thus, we found that the regulation levels of genes related to fatty acid synthesis were significantly higher in the fat line, suggesting the adipose tissues in fat birds have stronger ability of triglycerides synthesis in adipocytes.

4.3. Cholesterol synthesis

At the cellular level, the deposition of adipose tissue is the result of the increase of the number of adipocytes (adipogenesis) and the size of single fat cells (triglyceride and cholesterol accumulation in lipid droplets) [46,47].

Adipose tissue is the major site for the storage of cholesterol, containing both free and esterified forms of cholesterol [48]. In the current study, some critical DEGs (*EPHX2*, *POR*, and *HSD17B7*) and DAPs (ACAT1, EPHX2, POR, and HSD17B7) were related to cholesterol synthesis (Table 1). ACAT1 is an acetyl-coenzyme A acetyltransferase, which can catalyze the formation of cholesteryl esters from cholesterol and long-chain fatty acyl-CoAs [49]. EPHX2 is a member of the epoxide hydrolase family, and the N-terminal activity of EPHX2 can increase the cell's cholesterol level [50,51]. POR is a microsomal membrane-associated protein of two types: type I and type II, of which type II is responsible for cholesterol synthesis [52]. Lanosterol-14α-demethylase and squalene monooxygenase can participate in cholesterol biosynthesis and require POR as the electron donor [53,54]. HSD17B7 belongs to the 17β-hydroxysteroid dehydrogenase family that catalyze the conversion of the keto group on the 17th carbon in steroids to their 17β-hydroxy forms, and function as the 3-ketosteroid reductase of cholesterol biosynthesis [55].

In the present study, ACAT1, EPHX2, POR and HSD17B7 were all up-regulated in abdominal adipose tissue of fat line in the current study, suggesting the fat broilers could accumulate more cholesterol to expand the size of adipocytes.

4.4. Lipid droplet accumulation

Lipid droplets are dynamic organelles involved in intracellular lipid metabolism in almost all eukaryotic cells, and in white adipocytes, the large unique lipid droplet occupies most of the cell space and volume [56].

In the present study, PLIN1, PLIN4 and CAV1 associated with lipid droplet accumulation were up-regulated in FL compared with LL (Table 1). PLINs are proteins that coat lipid droplets in adipocytes, which control the lipolysis of stored neutral lipids by cytosolic lipases. PLIN1 is the most abundant lipid droplet coat protein, and plays a crucial role in restricting adipose lipolysis under basal or fed conditions [57]. PLIN4 mainly exists in white adipose tissue and is associated with tiny nascent lipid droplets. As a lipid droplet coat protein, PLIN4 can quickly package newly synthesized triacylglycerol, and store energy to the greatest extent during excessive nutrition [58]. Another lipid droplet

coat protein is CAV1, which is an essential component for the assembly of caveola organelles in highly differentiated cells, such as adipocytes. CAV1 usually plays a key structural role in the accumulation of lipid droplets in adipocytes, since the deletion of CAV1 can reduce lipid accumulation, which leads to progressive atrophy of white adipose tissue [59]. PLIN1, PLIN4 and CAV1 were up-regulated in the adipose tissue of fat line, indicating that fat birds may accumulate more lipid droplets in adipocytes than the lean birds.

For LL chickens, there are numerous down-regulated DEGs (*HEXB*, *CTSV*, *CLTA*, *ARSB*, *LAPTM5*, *DNASE2B*, *CTSC*, *CTSS*, *CTSH*, *ACP5*, *SLC11A1*, *LITAF*, *GM2A*, and *ATP6V0D2*) and DAPs (PPT1, NAGA, GNS, CTSS, CTSD, and GLA) significantly enriched in "lysosome" by KEGG analysis (Fig. 3b and Table 1). Lysosomes are small organelles (100–500 nm diameter) that contained proteasomes, lipases and nucleases [60]. Autophagy is closely related to lysosomes because it targets defective organelles to lysosomes for degradation [61]. Researchers reported that autophagy plays a complex role in adipose deposition. Zhao et al. [62] revealed that the activation of autophagy can suppress the adipogenesis of human adipose derived stem cells. Singh et al. [63] first reported the similarities in regulation and function between lipolysis and autophagy in hepatocytes such as autophagy is required for lipid droplet breakdown, and inhibition of autophagy will increase lipid storage. Another study showed inhibition of autophagy by Bisphenol A exposure will result in decreased lipid droplet degradation and increased ROS levels [64]. Other studies also showed that autophagy plays essential roles in lipolysis, which could eliminate fat [65,66], although many researches have shown that autophagy plays a positive role in adipocyte differentiation [67,68].

In the present study, numerous key DEGs and DAPs related to lysosome pathway were up-regulated in lean line, speculating that the autophagy-lysosome pathway was activated in the abdominal adipose tissue of lean birds, which promote lipolysis in adipocytes and reduce lipid droplet accumulation.

4.5. Adipose tissue and endocrine

Adipose tissue is not only viewed as a passive repository for triacylglycerol storage and a source of free fatty acids but as an active endocrine and paracrine organ secreting tissue, which through peptide hormones (adipokines) and non-peptide endocrine factor (cytokines, *etc.*) contribute to diverse metabolic processes including food intake, regulation of energy balance, insulin action, glucose and lipid metabolism, *etc.* [68,69].

A recent study reported the endocrine function of chicken visceral fat and found that some adipokines (such as *adipolin*, *ADIPOQ*, *ANGPT1* and *SFTPA1*) showed differences in mRNA expression level between fat and lean broilers [70]. However, in the present study, the expression of these adipokines did not show differences both at mRNA and protein levels between the fat and lean broiler lines, which may be overshadowed by the different sex or genetic background of the animal model. Nevertheless, in previous studies, people indicated that "cytokine-cytokine receptor interaction" pathway was related to fat deposition in chicken adipose tissue [71,72]. Specially, Cai et al. [73] reported that the "cytokine-cytokine receptor interaction" was the greatest down-regulation pathway in the inguinal white adipose tissue of obese mice compared with wild-type mice, which is consistent with our results.

In the present study, the "cytokine-cytokine receptor interaction" pathway was significantly enriched by up-regulated DEGs in our lean chickens (Fig. 3a), indicating that activation of this pathway and the involved genes might reduce the fat deposition in chicken abdominal fat tissue. Of course, systematic research on this topic is needed to solve the comprehensive functions of adipose tissue in endocrine regulation.

5. Conclusion

In summary, molecular differences related to long-chain fatty acid uptake, *in situ* lipogenesis (fatty acid and cholesterol synthesis), and lipid droplet accumulation were discovered to exist between the fat and lean chicken lines, which may contribute to the striking differences of abdominal fat deposition.

Through the joint analysis of transcriptome and proteome, we found many key genes that may affect chicken fat deposition (Table S7). The differential expression and molecular function of these genes likely lead to the differential accumulation of abdominal fat content, although some of them have not been reported to be directly related to adiposity, such as amino acid metabolism-related genes (ARL6IP5 and GSTT1L) and oxidation-reduction-related genes (PRDX6, RETSAT and VAT1) (Table S7). Functions of these genes in adipose tissue development and fat deposition await further investigation.

Supplementary data to this article can be found online at https://doi.org/10.1016/j.jprot.2021.104242.

Data availability

The transcriptomics datasets generated during the current study are available in NCBI SRA (PRJNA354990; SRR5055412 to SRR5055416 for FL and SRR5055375 to SRR5055379 for LL) and the mass spectrometry proteomics data have been deposited to the ProteomeXchange Consortium (http://proteomecentral.proteomexchange.org) *via* iProX (Integrated proteome resources, http://www.iprox.org/) with the dataset identifier PXD024710, and other data generated or analyzed during this study are included in this published article and its supplementary information files.

Authors contributions

L.J.W. performed the experiments, data curation, drafted and wrote the original manuscript. L.L., R.D. and C.L. participated in the sample collection and helped perform the experiments. P.F.G. participated in the data curation and visualization. N.W. helped design the study. H.L. contributed to funding acquisition and conceptualization. Z.Q.D. and B. H.C. contributed to the project administration, review and editing manuscript revision. All authors read and approved the final manuscript.

Declaration of Competing Interests

The authors declare that they have no competing interests.

Acknowledgments

The authors thank the members of Poultry Research Group in College of Animal Science and Technology at Northeast Agricultural University for hatching eggs and laboratory technical analyses. We also thank Shanghai Luming Biotech. Co. Ltd. for their assistance in the analysis of proteomic data.

The authors acknowledge funding for this study from China Agriculture Research System (No. CARS-41) and the National High-tech R&D Program of China (No. 2013AA102501).

References

[1] G.Q. Wu, X.M. Deng, J.Y. Li, N. Li, N. Yang, A potential molecular marker for selection against abdominal fatness in chickens, Poult. Sci. 85 (11) (2006) 1896–1899.

[2] F. Li, G. Hu, H. Zhang, S. Wang, Z. Wang, H. Li, Epistatic effects on abdominal fat content in chickens: results from a genome-wide SNP-SNP interaction analysis, PLoS One 8 (12) (2013), e81520.

[3] G. Hu, S.Z. Wang, Z.P. Wang, Y.M. Li, H. Li, Genetic epistasis analysis of 10 peroxisome proliferator-activated receptor γ-correlated genes in broiler lines divergently selected for abdominal fat content, Poult. Sci. 89 (11) (2010) 2341–2350.

[4] H. Ain Baziz, P.A. Geraert, J.C. Padilha, S. Guillaumin, Chronic heat exposure enhances fat deposition and modifies muscle and fat partition in broiler carcasses, Poult. Sci. 75 (4) (1996) 505–513.

[5] P.A. Geraert, J.C. Padilha, S. Guillaumin, Metabolic and endocrine changes induced by chronic heat exposure in broiler chickens: growth performance, body composition and energy retention, Br. J. Nutr. 75 (2) (1996) 195–204.
[6] F.R. Leenstra, Effect of age, sex, genotype and environment on fat deposition in broiler chickens—a review, World. Poult. Sci. J. 42 (1) (1986) 12–25.
[7] M. Alves-Bezerra, D.E. Cohen, Triglyceride metabolism in the liver, Compr. Physiol. 8 (10) (2017) 1–8.
[8] G. Wang, W.K. Kim, M.A. Cline, E.R. Gilbert, Factors affecting adipose tissue development in chickens: a review, Poult. Sci. 96 (10) (2017) 3687–3699.
[9] L. Guo, B. Sun, Z. Shang, L. Leng, Y. Wang, N. Wang, H. Li, Comparison of adipose tissue cellularity in chicken lines divergently selected for fatness, Poult. Sci. 90 (9) (2011) 2024–2034.
[10] H. Wang, H. Li, Q. Wang, Y. Wang, H. Han, H. Shi, Microarray analysis of adipose tissue gene expression profiles between two chicken breeds, J. Biosci. 31 (5) (2006) 565–573.
[11] H.B. Wang, H. Li, Q.G. Wang, X.Y. Zhang, S.Z. Wang, Y.X. Wang, X.P. Wang, Profiling of chicken adipose tissue gene expression by genome array, BMC Genomics 8 (2007) 193.
[12] D. Wang, N. Wang, N. Li, H. Li, Identification of differentially expressed proteins in adipose tissue of divergently selected broilers, Poult. Sci. 88 (11) (2009) 2285–2292.
[13] C.Y. Wu, Y.Y. Wu, C.D. Liu, Y.X. Wang, W. Na, N. Wang, H. Li, Comparative proteome analysis of abdominal adipose tissues between fat and lean broilers, Proteome Sci. 14 (1) (2016) 9.
[14] H. Zhang, H. Jiang, Y. Fan, Z. Chen, M. Li, Y. Mao, N.A. Karrow, J.J. Loor, S. Moore, Z. Yang, Transcriptomics and iTRAQ-proteomics analyses of bovine mammary tissue with *Streptococcus agalactiae*-induced mastitis, J. Agric. Food Chem. 66 (42) (2018) 11188–11196.
[15] W. Na, Y.Y. Wu, P.F. Gong, C.Y. Wu, B.H. Cheng, Y.X. Wang, N. Wang, Z.Q. Du, H. Li, Embryonic transcriptome and proteome analyses on hepatic lipid metabolism in chickens divergently selected for abdominal fat content, BMC Genomics 19 (1) (2018) 384.
[16] Y. Xu, H. Qian, X. Feng, Y. Xiong, M. Lei, Z. Ren, B. Zuo, D. Xu, Y. Ma, H. Yuan, Differential proteome and transcriptome analysis of porcine skeletal muscle during development, J. Proteome 75 (7) (2012) 2093–2108.
[17] D. Kim, B. Langmead, S.L. Salzberg, HISAT: a fast spliced aligner with low memory requirements, Nat. Methods 12 (4) (2015) 357–360.
[18] M. Pertea, G.M. Pertea, C.M. Antonescu, T.C. Chang, J.T. Mendell, S.L. Salzberg, StringTie enables improved reconstruction of a transcriptome from RNA-seq reads, Nat. Biotechnol. 33 (3) (2015) 290–295.
[19] M.I. Love, W. Huber, S. Anders, Moderated estimation of fold change and dispersion for RNA-seq data with DESeq2, Genome Biol. 15 (12) (2014) 550.
[20] C. Damerval, D. De Vienne, M. Zivy, H. Thiellement, Technical improvements in two-dimensional electrophoresis increase the level of genetic variation detected in wheat-seedling proteins, Electrophoresis 7 (1986) 52–54.
[21] M.M. Bradford, A rapid and sensitive method for the quantitation of microgram quantities of protein utilizing the principle of protein-dye binding, Anal. Biochem. 72 (1976) 248–254.
[22] I.V. Shilov, S.L. Seymour, A.A. Patel, A. Loboda, W.H. Tang, S.P. Keating, C. L. Hunter, L.M. Nuwaysir, D.A. Schaeffer, The paragon algorithm, a next generation search engine that uses sequence temperature values and feature probabilities to identify peptides from tandem mass spectra, Mol. Cell. Proteomics 6 (9) (2007) 1638–1655.
[23] J.T. Leek, W.E. Johnson, H.S. Parker, A.E. Jaffe, J.D. Storey, The sva package for removing batch effects and other unwanted variation in high-throughput experiments, Bioinformatics 28 (6) (2012) 882–883.
[24] B. MacLean, D.M. Tomazela, N. Shulman, M. Chambers, G.L. Finney, B. Frewen, R. Kern, D.L. Tabb, D.C. Liebler, M.J. MacCoss, Skyline: an open source document editor for creating and analyzing targeted proteomics experiments, Bioinformatics 26 (7) (2010) 966–968.
[25] G. Yu, L.G. Wang, Y. Han, Q.Y. He, clusterProfiler: an R package for comparing biological themes among gene clusters, Omics 16 (5) (2012) 284–287.
[26] S.M. Grundy, H.B. Brewer Jr., J.I. Cleeman, S.C. Smith Jr., C. Lenfant, American Heart Association, National Heart, Lung, and Blood Institute, Definition of metabolic syndrome: report of the National Heart, Lung, and Blood Institute/ American Heart Association conference on scientific issues related to definition, Circulation 109 (3) (2004) 433–438.
[27] H. Griffin, D. Hermier, Plasma lipoprotein metabolism and fattening in poultry, in: Leanness in Domestic Birds, 1988.
[28] M. Ramenofsky, Fat storage and fat metabolism in relation to migration, in: Bird Migration, 1990.
[29] D. Hermier, A. Quignard-Boulangé, I. Dugail, G. Guy, M.R. Salichon, L. Brigant, B. Ardouin, B. Leclercq, Evidence of enhanced storage capacity in adipose tissue of genetically fat chickens, J. Nutr. 119 (10) (1989) 1369–1375.
[30] J.E. Schaffer, H.F. Lodish, Molecular mechanism of long-chain fatty acid uptake, Trends Cardiovasc. Med. 5 (6) (1995) 218–224.
[31] K. Sato, Y. Akiba, Y. Chida, K. Takahashi, Lipoprotein hydrolysis and fat accumulation in chicken adipose tissues are reduced by chronic administration of lipoprotein lipase monoclonal antibodies, Poult. Sci. 78 (9) (1999) 1286–1291.
[32] B.L. Trigatti, R.G. Anderson, G.E. Gerber, Identification of caveolin-1 as a fatty acid binding protein, Biochem. Biophys. Res. Commun. 255 (1) (1999) 34–39.
[33] J. Pohl, A. Ring, R. Ehehalt, H. Schulze-Bergkamen, A. Schad, P. Verkade, W. Stremmel, Long-chain fatty acid uptake into adipocytes depends on lipid raft function, Biochemistry 43 (14) (2004) 4179–4187.
[34] T. Meshulam, J.R. Simard, J. Wharton, J.A. Hamilton, P.F. Pilch, Role of caveolin-1 and cholesterol in transmembrane fatty acid movement, Biochemistry 45 (9) (2006) 2882–2893.
[35] J.E. Schaffer, H.F. Lodish, Expression cloning and characterization of a novel adipocyte long chain fatty acid transport protein, Cell 79 (3) (1994) 427–436.
[36] C.E. Gargiulo, S.M. Stuhlsatz-Krouper, J.E. Schaffer, Localization of adipocyte long-chain fatty acyl-CoA synthetase at the plasma membrane, J. Lipid Res. 40 (5) (1999) 881–892.
[37] J. Krammer, M. Digel, F. Ehehalt, W. Stremmel, J. Füllekrug, R. Ehehalt, Overexpression of CD36 and acyl-CoA synthetases FATP2, FATP4 and ACSL1 increases fatty acid uptake in human hepatoma cells, Int. J. Med. Sci. 8 (7) (2011) 599–614.
[38] F. Tong, P.N. Black, R.A. Coleman, C.C. DiRusso, Fatty acid transport by vectorial acylation in mammals: roles played by different isoforms of rat long-chain acyl-CoA synthetases, Arch. Biochem. Biophys. 447 (1) (2006) 46–52.
[39] A. Stahl, A current review of fatty acid transport proteins (SLC27), Pflugers Arch. 447 (5) (2004) 722–727.
[40] G.A. Leveille, In vitro hepatic lipogenesis in the hen and chick, Comp. Biochem. Physiol. 28 (1) (1969) 431–435.
[41] C.W. Resnyk, W. Carré, X. Wang, T.E. Porter, J. Simon, E. Le Bihan-Duval, M. J. Duclos, S.E. Aggrey, L.A. Cogburn, Transcriptional analysis of abdominal fat in genetically fat and lean chickens reveals adipokines, lipogenic genes and a link between hemostasis and leanness, BMC Genomics 14 (2013) 557.
[42] C.W. Resnyk, C. Chen, H. Huang, C.H. Wu, J. Simon, E. Le Bihan-Duval, M. J. Duclos, L.A. Cogburn, RNA-Seq analysis of abdominal fat in genetically fat and lean chickens highlights a divergence in expression of genes controlling adiposity, hemostasis, and lipid metabolism, PLoS One 10 (10) (2015), e0139549.
[43] C.W. Resnyk, W. Carré, X. Wang, T.E. Porter, J. Simon, E. Le Bihan-Duval, M. J. Duclos, S.E. Aggrey, L.A. Cogburn, Transcriptional analysis of abdominal fat in chickens divergently selected on bodyweight at two ages reveals novel mechanisms controlling adiposity: validating visceral adipose tissue as a dynamic endocrine and metabolic organ, BMC Genomics 18 (1) (2017) 626.
[44] J.M. Collins, M.J. Neville, K.E. Pinnick, L. Hodson, B. Ruyter, T.H. van Dijk, D. J. Reijngoud, M.D. Fielding, K.N. Frayn, De novo lipogenesis in the differentiating human adipocyte can provide all fatty acids necessary for maturation, J. Lipid Res. 52 (9) (2011) 1683–1692.
[45] J.M. Ntambi, Regulation of stearoyl-CoA desaturase by polyunsaturated fatty acids and cholesterol, J. Lipid Res. 40 (9) (1999) 1549–1558.
[46] P.T. Kovanen, E.A. Nikkilä, T.A. Miettinen, Regulation of cholesterol synthesis and storage in fat cells, J. Lipid Res. 16 (3) (1975) 211–223.
[47] E.D. Rosen, B.M. Spiegelman, Adipocytes as regulators of energy balance and glucose homeostasis, Nature 444 (7121) (2006) 847–853.
[48] B.R. Krause, A.D. Hartman, Adipose tissue and cholesterol metabolism, J. Lipid Res. 25 (2) (1984) 97–110.
[49] C.J. Antalis, T. Arnold, B. Lee, K.K. Buhman, R.A. Siddiqui, Docosahexaenoic acid is a substrate for ACAT1 and inhibits cholesteryl ester formation from oleic acid in MCF-10A cells, Prostaglandins Leukot. Essent. Fat. Acids 80 (2–3) (2009) 165–171.
[50] A.E. EnayetAllah, A. Luria, B. Luo, H.J. Tsai, P. Sura, B.D. Hammock, D.F. Grant, Opposite regulation of cholesterol levels by the phosphatase and hydrolase domains of soluble epoxide hydrolase, J. Biol. Chem. 283 (52) (2008) 36592–36598.
[51] M.F. Domingues, N. Callai-Silva, A.R. Piovesan, C.R. Carlini, Soluble epoxide hydrolase and brain cholesterol metabolism, Front. Mol. Neurosci. 12 (2020) 325.
[52] A. Aguilar, S. Wu, F. De Luca, P450 oxidoreductase expressed in rat chondrocytes modulates chondrogenesis via cholesterol- and Indian hedgehog-dependent mechanisms, Endocrinology 150 (6) (2009) 2732–2739.
[53] T. Ono, K. Bloch, Solubilization and partial characterization of rat liver squalene epoxidase, J. Biol. Chem. 250 (4) (1975) 1571–1579.
[54] N. Debeljak, M. Fink, D. Rozman, Many facets of mammalian lanosterol 14alpha-demethylase from the evolutionarily conserved cytochrome P450 family CYP51, Arch. Biochem. Biophys. 409 (1) (2003) 159–171.
[55] Z. Marijanovic, D. Laubner, G. Moller, C. Gege, B. Husen, J. Adamski, R. Breitling, Closing the gap: identification of human 3-ketosteroid reductase, the last unknown enzyme of mammalian cholesterol biosynthesis, Mol. Endocrinol. 17 (9) (2003) 1715–1725.
[56] M. Konige, H. Wang, C. Sztalryd, Role of adipose specific lipid droplet proteins in maintaining whole body energy homeostasis, Biochim. Biophys. Acta 1842 (3) (2014) 393–401.
[57] C. Sztalryd, D.L. Brasaemle, The perilipin family of lipid droplet proteins: gatekeepers of intracellular lipolysis, Biochim. Biophys. Acta Mol. Cell Biol. Lipids 1862 (10 Pt B) (2017) 1221–1232.
[58] N.E. Wolins, B.K. Quaynor, J.R. Skinner, M.J. Schoenfish, A. Tzekov, P.E. Bickel, S3-12, Adipophilin, and TIP47 package lipid in adipocytes, J. Biol. Chem. 280 (19) (2005) 19146–19155.
[59] A.W. Cohen, B. Razani, W. Schubert, T.M. Williams, X.B. Wang, P. Iyengar, D. L. Brasaemle, P.E. Scherer, M.P. Lisanti, Role of caveolin-1 in the modulation of lipolysis and lipid droplet formation, Diabetes 53 (5) (2004) 1261–1270.
[60] Y. Mao, F. Yu, J. Wang, C. Guo, X. Fan, Autophagy: a new target for nonalcoholic fatty liver disease therapy, Hepatic Med.: Evid. Res. 8 (2016) 27–37.
[61] J.H. Hurley, B.A. Schulman, Atomistic autophagy: the structures of cellular self-digestion, Cell 157 (2) (2014) 300–311.
[62] L. Zhao, J.H. Ha, M. Okla, S. Chung, Activation of autophagy and AMPK by gamma-tocotrienol suppresses the adipogenesis in human adipose derived stem cells, Mol. Nutr. Food Res. 58 (3) (2014) 569–579.

[63] R. Singh, S. Kaushik, Y. Wang, Y. Xiang, I. Novak, M. Komatsu, K. Tanaka, A. M. Cuervo, M.J. Czaja, Autophagy regulates lipid metabolism, Nature 458 (7242) (2009) 1131–1135.
[64] D. Song, Y. Chen, B. Wang, D. Li, C. Xu, H. Huang, S. Huang, R. Liu, Bisphenol a inhibits autophagosome-lysosome fusion and lipid droplet degradation, Ecotoxicol. Environ. Saf. 183 (2019) 109492.
[65] R. Zechner, F. Madeo, Cell biology: another way to get rid of fat, Nature 458 (7242) (2009) 1118–1119.
[66] A. Lizaso, K.T. Tan, Y.H. Lee, β-adrenergic receptor-stimulated lipolysis requires the RAB7-mediated autolysosomal lipid degradation, Autophagy 9 (8) (2013) 1228–1243.
[67] W. Zhang, P. Li, S. Wang, G. Cheng, L. Wang, X. Mi, X. Su, Y. Wang, L. Zan, TP53INP2 promotes bovine adipocytes differentiation through autophagy activation, Animals 9 (12) (2019) 1060.
[68] D.C. Lau, Adipose tissue growth and differentiation: view from the chair, Int. J. Obes Relat. Metab. Disord. 24 (Suppl_4) (2000) S20–S22.
[69] P. Ferroni, S. Basili, A. Falco, G. Davì, Inflammation, insulin resistance, and obesity, Curr. Atheroscler. Rep. 6 (6) (2004) 424–431.
[70] S. Bornelöv, E. Seroussi, S. Yosefi, S. Benjamini, S. Miyara, M. Ruzal, M. Grabherr, N. Rafati, M. Molin, A.K. Pendavis, C. Burgess, S.L. Andersson, M. Friedman-Einat, Comparative omics and feeding manipulations in chicken indicate a shift of the endocrine role of visceral fat towards reproduction, BMC Genomics 19 (1) (2018) 295.
[71] F. Qiu, L. Xie, J.E. Ma, W. Luo, L. Zhang, Z. Chao, S. Chen, Q. Nie, Z. Lin, X. Zhang, Lower expression of SLC27A1 enhances intramuscular fat deposition in chicken via down-regulated fatty acid oxidation mediated by CPT1A, Front. Physiol. 8 (2017) 449.
[72] L. Liu, H.X. Cui, M.Q. Zheng, G.P. Zhao, J. Wen, Comparative analysis of differentially expressed genes related to triglyceride metabolism between intramuscular fat and abdominal fat in broilers, Br. Poult. Sci. 59 (5) (2018) 514–520.
[73] R. Cai, G. Tang, Q. Zhang, W. Yong, W. Zhang, J. Xiao, C. Wei, C. He, G. Yang, W. Pang, A novel lnc-RNA, named lnc-ORA, is identified by RNA-Seq analysis, and its knockdown inhibits adipogenesis by regulating the PI3K/AKT/mTOR signaling pathway, Cells 8 (5) (2019) 477.